## PHYSICS OF ELEMENTARY PARTICLES AND ATOMIC NUCLEI. EXPERIMENT

# Assembly Device for Supermodules of Silicon Tracking System of the BM@N Experiment

**V. V. Elsha[a], M. G. Korolev[b], D. V. Dementev[a], \*, S. N. Igolkin[c], N. V. Sukhov[a], A. D. Sheremetev[a], M. O. Shitenkow[a], A. L. Voronin[a], and Yu. A. Murin[a]**

[a] Veksler and Baldin Laboratory of High Energy Physics, Joint Institute for Nuclear Research,
Dubna, Moscow oblast, 141980 Russia

[b] Skobeltsyn Institute of Nuclear Physics, Moscow State University, Moscow, 119991 Russia

[c] St. Petersburg University, St. Petersburg, 199034 Russia

*e-mail: dementiev@jinr.ru

Received December 18, 2022; revised January 13, 2023; accepted January 13, 2023

**Abstract**—The silicon tracking system of the BM@N experiment consists of four stations based on double-sided microstrip silicon sensors. The sensors make it possible to obtain a spatial resolution for tracks of secondary charged particles up to 17 μm. Two ASIC boards, the input channels of which are connected to the strips with ultralight (0.23% $X_0$) aluminum flex cables, are used to readout and process signals from both sides of the sensor. Such an assembly is called a module. Silicon sensors are mounted on lightweight carbon-fiber support trusses in a way that the dead zones at the edges are overlapped due to the tiled layout. The frontend electronics are housed in metal containers with a heat sink system located at the rare ends of the carbon-fiber support truss. A set of modules attached to the carbon-fiber support truss with two containers with readout electronics at the ends is called a supermodule. The accuracy of the sensor positioning in the station plane plays a crucial role in limiting the degrees of freedom of the parameters determined by the software during the final alignment of the tracking system elements. A special device that allows mounting sensors on a carbon fiber truss with an accuracy of up to 15 μm on a 1200 mm base is developed to assemble supermodules. The results of testing the device are given.

## INTRODUCTION

The silicon tracking system (STS) is one of the key elements of the facility, which is planned to be put into operation in the process of upgrading the detector systems of the Baryonic Matter at the Nuclotron experiment (BM@N) [1]. The improvement of the BM@N facility is aimed at solving the physical problem of studying the properties of superdense baryonic matter generated in collisions of heavy ions (up to $^{197}Au^{79+}$ gold nuclei) at energies up to 4.65 GeV per nucleon. The STS will include four stations based on track modules with double-sided silicon microstrip sensors [2]. The stations will be installed between the poles of the SP-41 dipole magnet inside the thermally insulated housing of the STS with built-in elements of water and gas cooling systems. The problems of STS are the reconstruction of the trajectories of secondary charged particles in order to determine the peaks of their production and their momenta. The layout of the STS and its main components is shown in Fig. 1.

The basic element of the STS is a track module [3], which consists of a double-sided silicon microstrip sensor, two boards with frontend electronics for reading out signals from both sides of the detector, and a set of ultralight flat aluminum cables on a polyimide basis (Fig. 2). The cables are used to transmit the analog signal from the sensor strips to the inputs of the reading chip. This design of the module makes it possible to create position-sensitive systems of a large area, allowing one to place the frontend electronics in the peripheral area of the stations. Such an arrangement of stations, in turn, makes it possible to minimize the amount of matter with which secondary particles interact when passing through the track system. Each double-sided microstrip STS sensor has 1024 strips on each side arranged with a step of 58 μm. On the N side of the sensor, the strips are directed strictly along the direction of the magnetic field, i.e., parallel to the edges of the sensor. On the P side of the sensor, the strips are positioned at an angle of 7.5° with respect to the strips on the opposite side. The initial design of the STS module was developed in the context of cooperation between the JINR and GSI working groups for the CBM collaboration (FAIR, Darmstadt, Germany) [4]. The design of the STS module was technologically redesigned by the JINR working
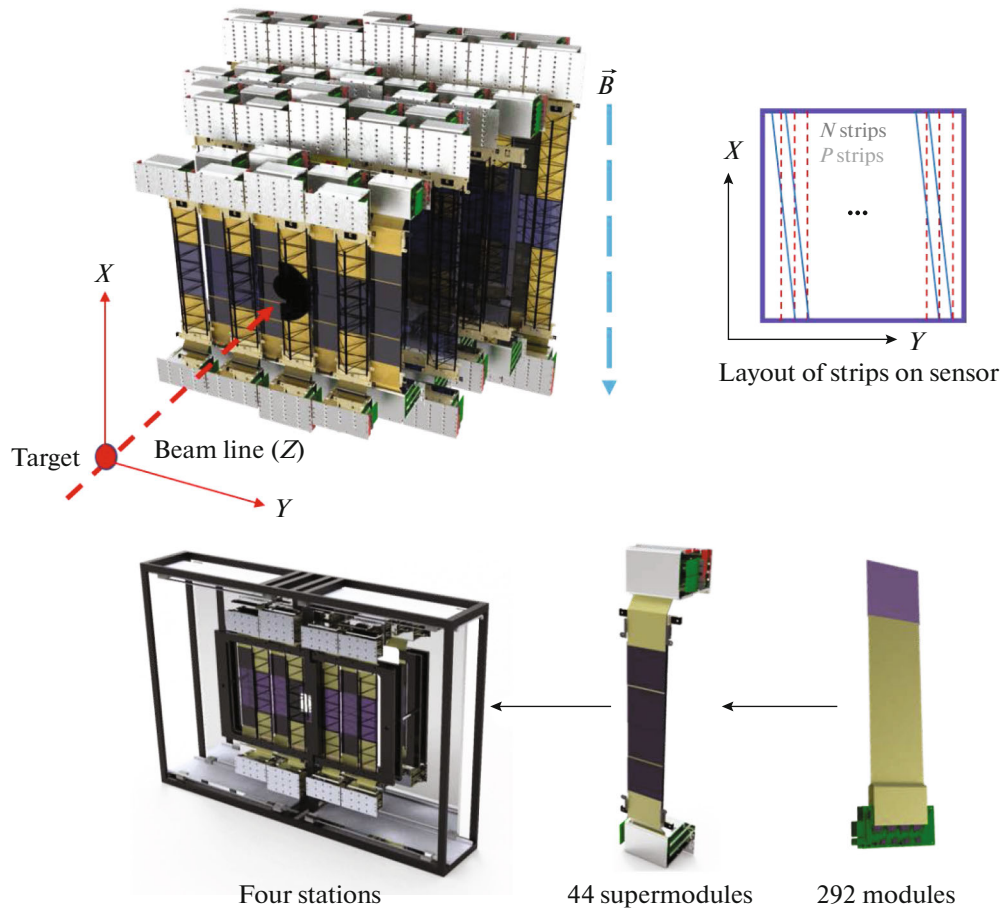
**Fig. 1.** Schematic representation of the main components of STS. The direction of the beam and coordinate axes and the orientation of the magnetic field of the dipole magnet, inside which the STS is located, are shown. The orientation of strips on microstrip sensors is schematically shown.
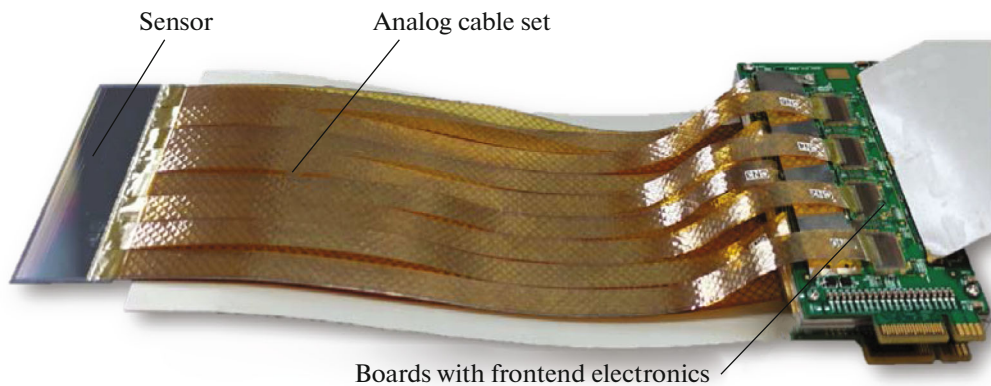


**Fig. 2.** Photo of the assembled STS BM@N module.

group without changing the basic concept according to the specific requirements of the BM@N experiment.

The STS consists of 292 modules of different sizes and forms 598 000 reading channels [5]. The module size is determined by the size of the sensor and the length of the cable connecting the detector strips to the input channels of the frontend electronics. In order to equalize the loading of the strips, the size of the sensors located in the zones of small scattering angles, i.e., close to the ion guide, are $42 \times 62$ mm$^2$. Sensors

with size of $62 \times 62$ mm$^2$ are installed at the periphery of track stations, where loads are relatively small. Modules of different sizes are placed on lightweight carbon-fiber support trusses. Such an assembly is called a supermodule.

The STS module is capable of providing a spatial resolution of up to $58/\sqrt{12} \approx 17$ μm. In practice, the accuracy of restoring the coordinates of secondary particles is determined not only by the resolution of the sensors, but also by the accuracy of their positioning in the supermodule and in the station. During the calibration of the track system, errors due to the inaccurate placement of elements of the track planes can be compensated using mathematical algorithms for the final adjustment of the system or alignment. These algorithms are based on the principle of minimizing the residual values for a large number of reconstructed particle tracks in when there is no a magnetic field [6]. The algorithm minimizes the given objective function by the least squares method. In the general case, it depends on the equalization corrections $\Delta p$ and track parameters $q$ [7]

$$F\left(\Delta p, q\right) = \sum_{\text{datasets}} \left( \sum_{\text{events}} \left( \sum_{\text{tracks}} \left( \sum_{\text{hits}} (\Delta_i^2/\sigma_i^2) \right) \right) \right), \quad (1)$$

where track discrepancy $\Delta_i$ is the difference between the found position of the hit (sensor response as a result of interaction with the particle) as a result of trajectory fitting and its measured coordinate, and $\sigma_i$ is the standard deviation of the measurement. Due to the large number of parameters, some of which correlate with each other, the minimization of objective function (1) is a difficult task, often leading to ambiguous results. The only way to improve the results of the adjustment algorithms is to reduce the ranges of possible parameter variations. In addition, the number of parameters for the final adjustment of the system is about $10^3$ due to the large number of sensors used in the BM@N tracking system, which, given the existing efficiency of the algorithms, may require an analysis of about $10^6$ tracks. The amount of data and the number of parameters for weakly defined degrees of freedom can be a problem even for modern computers.

In order to limit the degrees of freedom of the final adjustment parameters, it is necessary to ensure that the positioning accuracy of the track plane sensors during the detector assembly is no worse than $\pm100$ μm in the station plane orthogonal to the magnetic field lines.

The purpose of this work is to develop a technological process for assembling a STS supermodule with an accuracy of $\pm15$ μm in the mutual positioning of the sensors in a direction significant for the accuracy of measuring the particle momentum on a support truss with a length of up to 1200 mm. This accuracy is due to the possibilities of production and is sufficient for the effective alignment of the track system. In addi-

tion, such an accuracy of mutual positioning of sensors makes it possible to combine strips of adjacent sensors into a single chain to minimize channels of frontend electronics in areas with low loads. To solve this problem, we proposed an original procedure for assembling supermodules and created and tested a special device for assembling them, as well as a set of accessories and software for controlling the operation of the device.

## BM@N STS SUPERMODULE

In order to form a sensitive plane of a large area, the supermodules are mechanically combined in a STS node called a station. Supermodules of STS (depending on which station they are located in) contain from four to ten sensors. The design of the supermodule is shown in Fig. 3.

Supermodules are mounted vertically on the supporting structure of the station (i.e., coaxially with the direction of the magnetic field of the dipole magnet). In this case, strips of the same name on the N sides of all sensors installed on the supermodule must be located coaxially with an accuracy no worse than the spatial resolution of the sensors.

The central part of the supermodule is a set of sensors of different sizes and a stack of flat lightweight cables mounted on a carbon-fiber support truss. Each sensor has a security zone around its perimeter that is not coordinate-sensitive. The width of the zone is 1 mm. In order to avoid the dead zones, i.e., insensitive zones in the track planes, the sensors are arranged in the form of tiles with an overlap of 2.5 mm in the direction along the support truss. To do this, each sensor is attached to the support truss using the so-called L legs at a given height from the front side of the truss along which they are located. L legs are made of fiberglass in molds and glued with their short side to the sensor surface at the last stage of module assembly using specialized equipment [8]. The long side of the L leg is glued to the support truss of the supermodule at the last stage of its assembly described below.

The use of an ultralight carbon-fiber support truss for mounting sensors in the central part of the supermodule makes it possible to minimize the amount of substance in the sensitive area of the detector, as well as minimize the additional error in coordinate measurement caused by changes in the dimensions of the truss due to ambient temperature fluctuations.

The carbon-fiber support truss is made from M55J high modulus carbon fiber prepreg in molds. After the workpiece has cooled down, the truss geometry is leveled by additional heat treatment on precision granite. The weight of the truss is no more than 15 g per 1 m of length. The technology for manufacturing ultralight carbon composite trusses of this type, originally developed for the ALICE ITS detector (CERN) [9], was
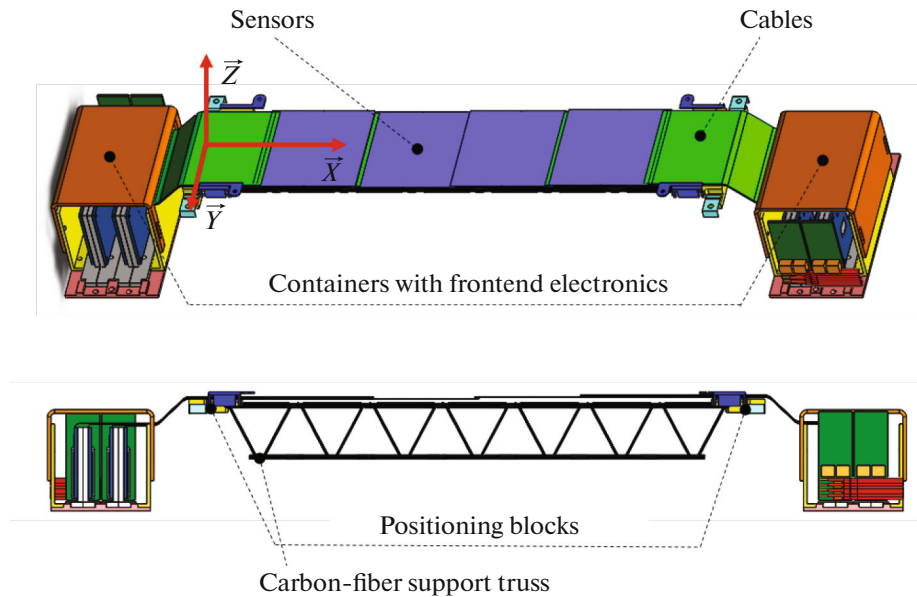
**Fig. 3.** Model of the STS supermodule.

successfully applied to manufacture modified BM@N STS trusses.

Containers at both ends of the supermodule serve to house the boards with the frontend electronics of the detector. They are made of aluminum alloys and interconnected by heat-conducting compounds for efficient heat removal from the frontend electronics of the detector to the heat exchangers of the liquid cooling system of the STS. Precise positioning in the station of these relatively massive elements is not required. The central part of the supermodule with sensors and containers with frontend electronics are interconnected only by a stack of thin analog cables, while there is no rigid mechanical connection between the parts. The central part of the supermodule is positioned on the carbon-fiber support structure of the station with high accuracy, and the containers with frontend electronics are mounted on the aluminum heat exchangers of the station.

Each truss has positioning units at the ends with a socket, the counterpart of which is a ruby ball on the stylus (Fig. 4). The stylus is mounted on the station plane, while the ruby balls unambiguously determine the position of the sensors in the station plane. It has been experimentally confirmed that the repeatability of supermodule positioning when using the specified attachment is $\pm 2$ μm. The position of each ruby ball relative to the fiducial points of the station is determined by the accuracy of the machine on which the mounting holes for the stylus are drilled and is about $10-15$ μm. The anchor point of the supermodule coordinate system is a ruby ball inserted into the connector of the positioning unit. This unit is located at one end of the support truss and has a V profile. The

positioning unit at the other end of the truss (SQ) determines the installation axis of the supermodule and has an oblong hole with a width equal to the diameter of the ball inserted into it. This design allows one to compensate for possible minor thermal fluctuations in the length of the truss and eliminate the mechanical stress caused by these fluctuations. STSs are based on trusses of three standard sizes with different distances between ruby balls at both ends (294.6, 414.6, and 538.6 mm).

## ASSEMBLY DEVICE FOR SUPERMODULES

The complexity of the technological process of assembling the BM@N STS supermodules is determined primarily by the need to position the silicon sensors on the truss with the maximum achievable accuracy for the dimensions of the object being assembled. It should be

(1) $\pm 15$ μm on 1200 mm base along $Y$ axis.

(2) $\pm 12$ μm on 180 mm base along $Y$ axis.

(3) $\pm 50$ μm along $X$ and $Z$ axes.

The designations of the coordinate axes are shown in Fig. 3. The increased accuracy of sensors installation on the truss in the direction orthogonal to the direction of the strips on the N side (requirement 2) comes from the need to ensure the alignment of the same-name strips of different sensors of the supermodule into a single superstrip of the supermodule directed along the magnetic field. Combining several sensors using aluminum loops connecting coaxial strips of different sensors allows a multiple reduction in the number of frontend electronics channels in zones with low loads. To use connecting aluminum
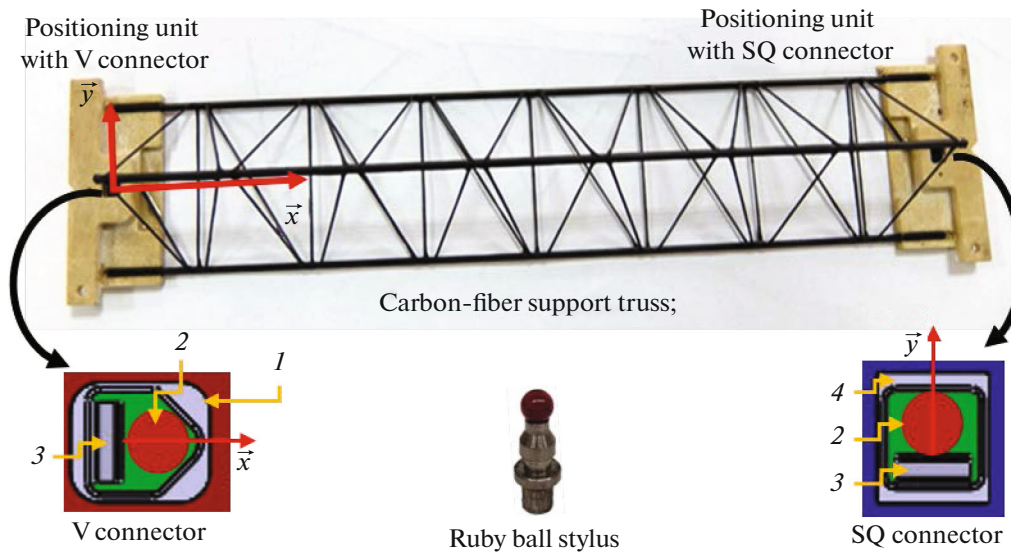
**Fig. 4.** Carbon-fiber support truss of the supermodule with positioning units. The ruby ball stylus used to position the supermodule in the station and the connectors of the V and SQ positioning units are shown at the bottom of the figure. The numbers indicate ( *1*) the titanium socket of the V connector, (*2*) the position of the ruby ball in the socket after the truss is installed in the station, (*3*) the hold-down spring, and (*4*) the titanium socket of the SQ connector.

loops, it is necessary to ensure the accuracy of the mutual positioning of the sensors no worse than 15 μm. An accuracy of 12 μm on a 180 μm base is chosen taking into account the possibilities of production.

It is obvious that ensuring the specified accuracy of sensor installation on an ultralight supporting truss when assembling supermodules is impossible without the manufacture of specialized precision equipment and the development of an appropriate technological process.

The assembly of the supermodule takes place in two stages on a specialized assembly device (AD). First, the sensors are placed on a precision bench with vacuum suction cup platforms, the position of which on the AD bench is adjusted by the operator until all assembly fiducial points are aligned with the specified table coordinates. A carbon-fiber support truss is placed in a similar way, the role of fiducial points of which is played by ruby balls in the sockets of positioning units. The balls imitate the position of the balls installed on the truss of the station for which the supermodule is assembled and on which its V and SQ positioning units will be mounted when the supermodule is installed in the station. Each sensor has eight fiducial marks on the surface applied to the surface of the crystal using photolithography by the manufacturer. The fiducial mark binding accuracy relative to the position of the strips on the sensor surface is ±0.1 μm. Thus, the accuracy with which the relative position of the marks and strips on the surface of the sensors is determined can be conditionally considered ideal, and the mutual position of the sensors in the assembly is due solely to the accuracy of the assembly

equipment and the work of the operator. A map of the position of the fiducial marks on the surface of the sensors and ruby balls in the truss positioning blocks was compiled for each size of the supermodule.

The work of the AD operator consists of the sequential iterative alignment of the position of each sensor with glued L legs and the truss relative to the tabular coordinates indicated using the AD target camera. The mechanical system for moving the AD target camera controlled by a computer program provides an accuracy of 2 μm. Then, at the second stage of supermodule assembly, drops of glue are applied between all L legs of the sensors and the truss. As a result, after the polymerization of the glue in one process, the specified relative position of the sensors and the truss is fixed.

This concept was implemented by us together with the engineers of Planar (Minsk, Belarus), at whose enterprise the AD was built. The AD scheme and its components are shown in Fig. 5.

The base of the facility is a granite plate, the weight of which is 600 kg. The use of a massive base allows one to avoid vibrations during the assembly of the supermodule. The device itself is located in a room equipped with climatic equipment, which allows one to maintain a constant temperature in the range of $22 \pm 2°C$.

There are two positioning systems on the granite plate. The first one serves to place the assembly template of the supermodule, which consists of a set of vacuum platforms for sensors. The second one is used for positioning the carbon-fiber support truss.
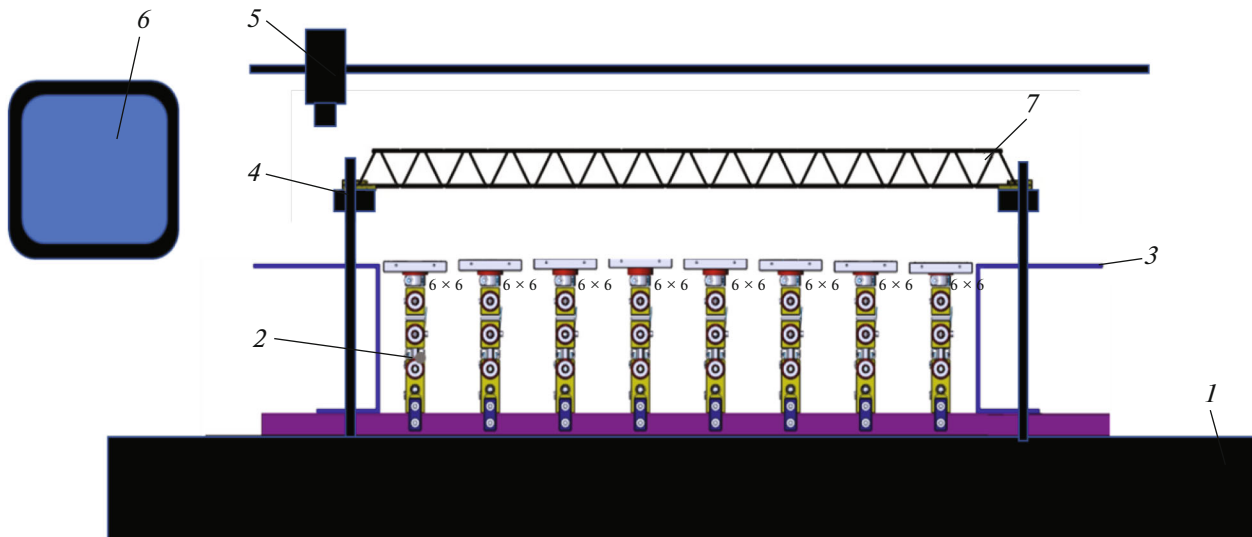
**Fig. 5.** Schematic representation of the AD. Numbers indicate (*1*) granite plate, (*2*) super module template consisting of vacuum platforms for sensors, (*3*) supports for cables and boards with detector frontend electronics, (*4*) crane for installing a carbon-fiber support truss with ruby balls for positioning units, (*5*) optical system with a linear movement system, (*6*) PC, and (*7*) carbon-fiber support truss.

Assembly templates of the supermodules are vacuum platforms for sensors assembled on a rail, and each platform is equipped with a three-coordinate manipulator. In the orthogonal coordinate system of the manipulator, the $X$ and $Y$ axes lie in the sensor (module) plane, while the $X$ axis is directed along the supermodule; angle $\Phi$ corresponds to the angle between the module axis and the $X$ axis. In total, up to 20 such platforms with manipulators can be installed, and they can accommodate sensors sized $62 \times 22$, $62 \times 42$, and $62 \times 62$ mm$^2$. To ensure overlap, the sensors on the supermodule are located at different distances from the truss, which is determined by the height of the platform ($Z$ axis). The height of the platform is adjustable in 1-mm increments. The vacuum for each platform can be supplied by a separate switch.

A three-coordinate targeting camera movement system with a spatial resolution of $\pm 2$ μm is located above the assembly. Software algorithms, whose parameters are calibrated using the built-in interference optical ruler, are used to compensate for the nonlinearity of camera movement systems. The backlash compensation of mechanical movement systems is also implemented using software. The movement of the camera to each point is performed according to a given algorithm with a fixed direction of movement. A photograph of the assembled device is shown in Fig. 6.

During the sequential placement of modules on the assembly template, the positions of the two selected fiducial marks on the module sensor are aligned with the corresponding points of the placement map for the selected template. At the same time, the optical system of the AD sequentially transmits the image of the position of two selected points of the map to the PC screen, and the operator iteratively moves the sensor fixed on the corresponding positioner of the assembly template with manual $X$, $Y$, and $\Phi$ manipulators, achieving the maximum alignment of the visible micromarks on the sensor with their desired calculated position. An example of running of the program is shown in Fig. 7.

The fiducial marks of the assembly have different sizes; the characteristic size of the crosses on the sensors is 50 μm and the diameter of the ruby balls is 4 mm. Therefore, the target camera is used at different magnifications when recognizing these objects. To avoid errors due to the changing of the position of the optical axis, two fixed zoom positions are used. The maximum magnification is applied for crosses, and the minimum magnification is applied for balls with mutual calibration of the position. The sharpness of the camera is changed by linear movements along the $Z$ axis tied to the height of each platform, and thus changes automatically when the camera moves from sensor to sensor.

The AD software performs the following functions:

• arbitrary movement of the target camera between the fiducial marks of the model selected by the operator from the set of fiducial marks of the assembled supermodule;

• recognition of the ruby ball and determination of its center to place the support truss in the gluing position;

• recognition of the fiducial mark on the sensor and measurement of the difference between the current coordinate and its design position;
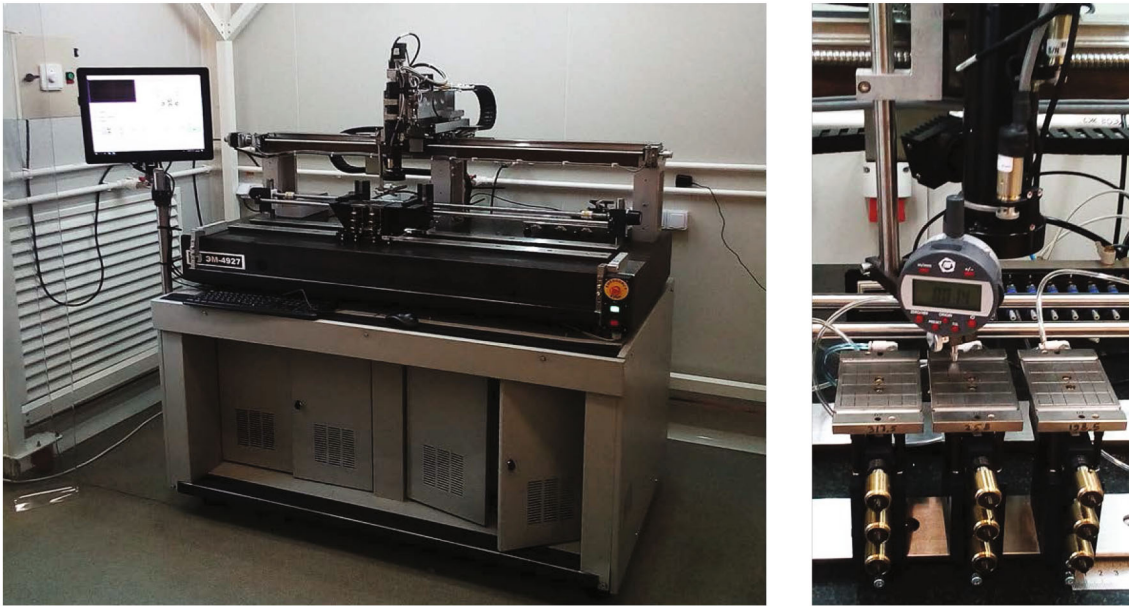
**Fig. 6.** Photo of AD (left) and photo of platforms for sensors with adjusting screws and target camera lens with fixed micrometer (right).
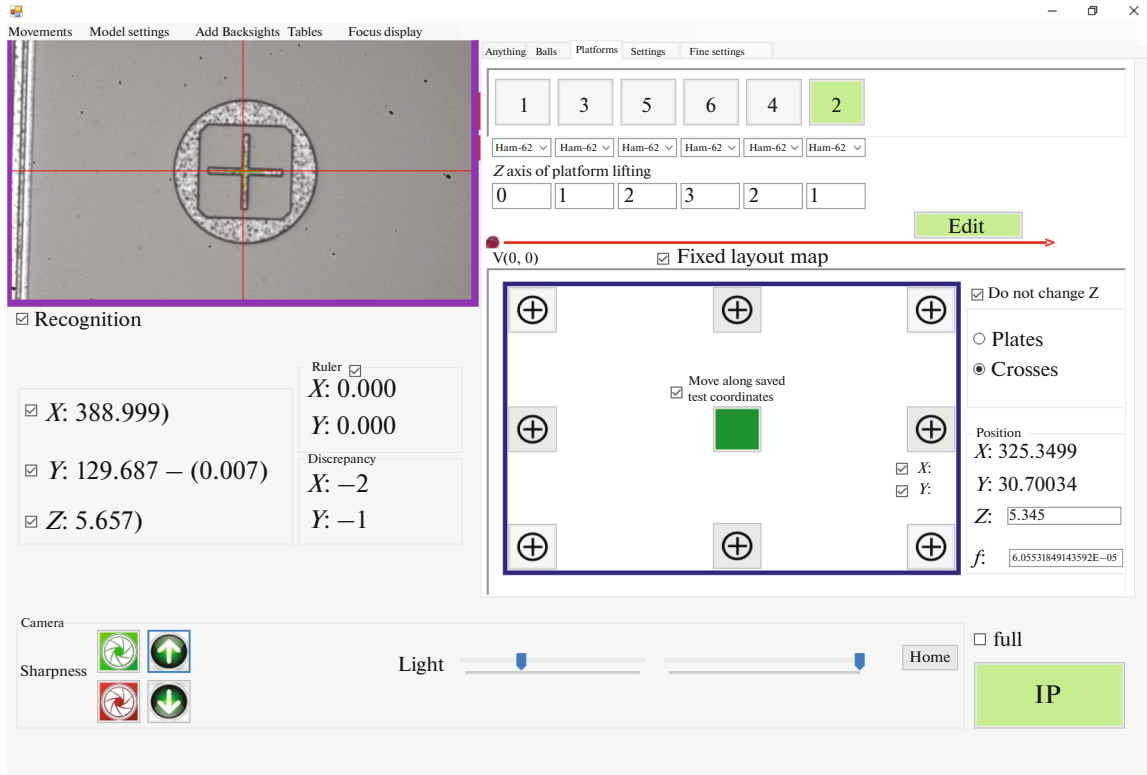


**Fig. 7.** Interface of the AD working program. The fiducial mark on the sensor surface is shown in the upper left corner; the red cross indicates the location of the mark according to the map. Values of coordinate discrepancy are given in micrometers.
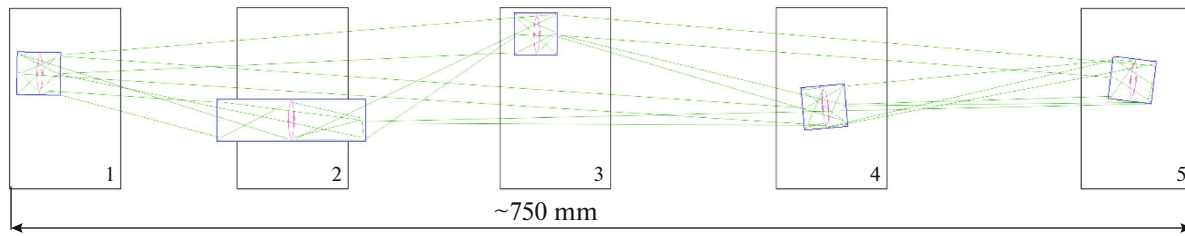
**Fig. 8.** Map of movements during the test measurements on the AD. The location of the vacuum platforms is shown in black; the position of the microcircuits (MCs) on the platforms is shown in blue. Movements between marks on different MCs are shown in green; consecutive movements between two marks on the same MCs are shown in red.

• software compensation for premeasured systematic nonlinearities in the movement system of the target camera;

• exit to the fiducial point specified by the operator with compensation of mechanical backlashes in the linear movements of the target camera;

• editing the coordinates of fiducial points of the supermodule, saving them to a file, and loading from a file;

• saving in the log file the deviations of the positions of the fiducial marks from their position in the model.

## RESULTS AND DISCUSSION

AD operation and the complete technological process of assembling the STS supermodules were tested first when assembling weight and size templates and then using several prototypes of the STS supermodules.

Templates with sets of vacuum platformes for sensors were assembled and adjusted to assemble the STS supermodules selected for prototyping. The AD is equipped with a micrometer stand that moves with the camera to initially align the assembly platforms in the $XY$ plane and check their heights ($Z$). The flatness of each platform was adjusted by spacers in their supports with an accuracy of $\pm 10$ μm.

The following measurements were carried out to check the repeatability of the positioning of the AD target camera. Five microcircuits (MCs), each one with eight fiducial marks, were used as prototypes. Each MC was on its own positioner platform. The microcircuits were prealigned on the plane of the platform to test the program for recognizing the center of the fiducial mark. The platforms were located at a distance of up to 200 mm from each other along the $X$ axis. The maximum movement of the camera was 750 mm. The coordinates of all 40 fiducial points of the deployed MCs were stored in memory as a spread map. The map of points and the scheme of movements of the target camera under subsequent measurements are shown in Fig. 8.

At the first stage of measurements, 100 movements between randomly selected marks were made. In the process of measurements, the difference in $X$ and $Y$ coordinates between the stored values of the map coordinates and the recognized mark position reached at the end of the movement was recorded. Table 1 shows the standard deviations for the $X$ and $Y$ coordinates of the marks for different ranges of movement of the target camera. The result is practically indepen-

**Table 1.** Repeatability of the results of measuring the coordinates of the fiducial marks using AD target camera at different ranges of the coordinate ruler. The description of measurements is given in the text

| Target camera range | $\sigma_x$, μm | $\sigma_y$, μm |
|---|---|---|
| $X$ axis range: 0−20 mm (within MC1) | 1.9 | 1.8 |
| $X$ axis range: 200−220 mm (within MC2) | 0.9 | 0.9 |
| $X$ axis range: 380−400 mm (within MC3) | 1.2 | 2.1 |
| $X$ axis range: 600−620 mm (within MC4) | 1.2 | 1.3 |
| $X$ axis range: 700−750 mm (within MC5) | 1.6 | 1.2 |
| $X$ axis range: 0−220 mm (between MC1 and MC2) | 1.9 | 2.0 |
| $X$ axis range: 200−400 mm (between MC2 and MC3) | 1.6 | 1.2 |
| $X$ axis range: 380−620 mm (between MC3 and MC4) | 1.9 | 2.3 |
| $X$ axis range: 600−750 mm (between MC4 and MC5) | 2.1 | 1.1 |
| $X$ axis range: 0−750 mm (between MC1 and MC5) | 1.8 | 1.7 |
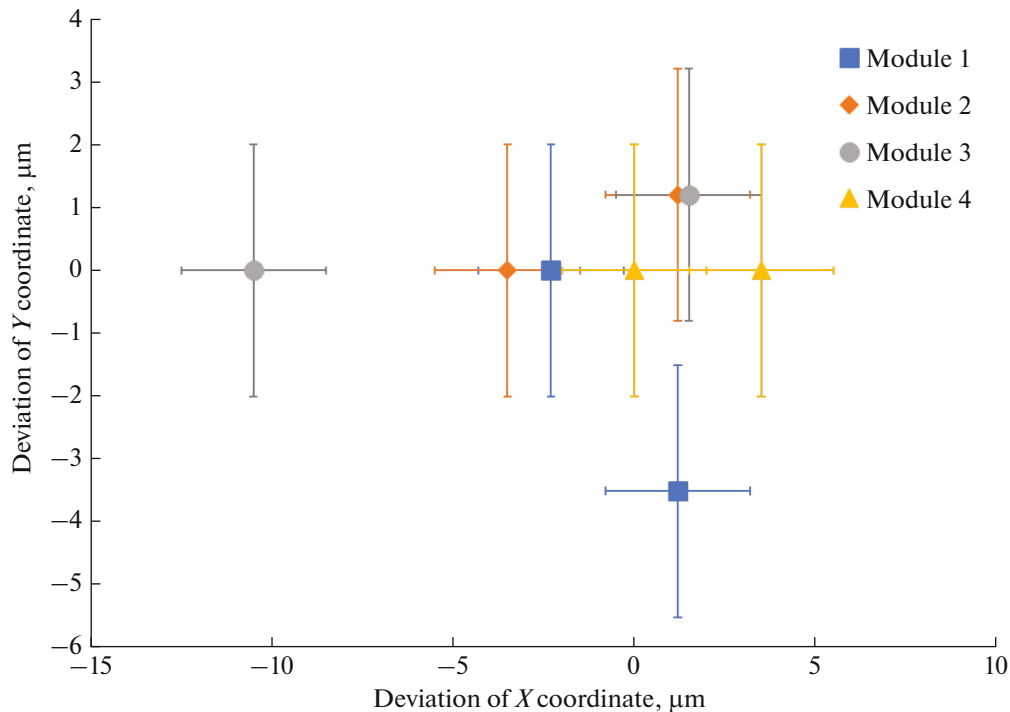
**Fig. 9.** Measured discrepancy between the coordinates of the marks on the sensors from the given positions on the map after assembling the supermodule with four modules. The $X$ axis is directed along the strips on the N sides of the sensors, and the $Y$ axis is directed perpendicular to the strips.

dent of the range of motion of the camera. The existing scatter of the measured values for different MCs is determined primarily by the parallelism of the platform plane to the plane of movement of the target camera. The maximum deviation of the measured coordinates along the $X$ and $Y$ axes from the mean values does not exceed 5 μm. On average, the standard deviation for both coordinates is $\sigma_{x,y} = 1.6$ μm for all measurements. The results are within the requirements.

At the next stage of measurements, iterative camera movements were simulated during the sensor alignment procedure. When performing this procedure, the operator performs a series of sequential movements of the camera between points on one sensor, performing point adjustment of the module position using the adjusting screws on the vacuum platform. In these measurements, the fidelity of coordinate reproduction was evaluated for ten successive movements between two marks on one MC. The selected points were located at different distances from each other. The movement pattern is shown in red in Fig. 8. The maximum deviation of both coordinates was 4 μm. It was shown that the repeatability of the camera positioning in these measurements is determined primarily by the parallelism of the platform surface to the camera movement plane. For platforms whose plane parallelism was preadjusted with an accuracy of ±10 μm, the repeatability of camera positioning was ±3 μm.

A series of successive measurements of the position of the center of the ball after moving the camera was carried out to check the quality of recognition of ruby balls at the ends of the trusses. The repeatability of the results was ±2 μm, which does not exceed the spatial resolution of the optical system.

The mass-size model of the supermodule of the first station of the STS including four sensors $62 \times 62$ mm² in size was assembled to check the technological process. The control measurement of the positions of the fiducial marks on the sensors was carried out after gluing the layout and polymerizing the glue. The measured values of the coordinates were compared with the line map. The results are shown in Fig. 9. Deviations of the position of the marks from the specified values do not exceed ±12.5 μm along the $X$ axis and ±6 μm along the $Y$ axis.

## CONCLUSIONS

We have developed a device that allows one to assemble supermodules for silicon track systems based on microstrip sensors with a positioning accuracy of detecting elements up to 15 μm on a 1200 mm base. The high positioning accuracy of the sensors will make it possible to significantly simplify the algorithms and increase the reliability of the final alignment of the track system elements of the facility. It is planned to use the assembly device and the procedure for install-

ing sensors to assemble all STS supermodules of the BM@N experiment.

## CONFLICT OF INTEREST

The authors declare that they have no conflicts of interest.

## REFERENCES

1. P. Senger, D. Dementev, J. Heuser, M. Kapishin, E. Lavrik, Y. Murin, A. Maksymchuk, H. R. Schmidt, C. Schmidt, A. Senger, and A. Zinchenko, "Upgrading the baryonic matter at the Nuclotron experiment at NICA for studies of dense nuclear matter," Particles **2**, 481−490 (2019).

2. D. Dementev, A. Baranov, V. Elsha, et al., "The silicon tracking system as a part of hybrid tracker of BM@N experiment," Phys. Part. Nucl. **53**, 197−202 (2022).

3. A. Sheremetiev, D. Dementev, V. Elsha, A. Kolozhvari, Y. Murin, M. Shitenkov, and N. Sukhov, "Status of the BM@STS module assembly," Phys. Part. Nucl. **53**, 377−381 (2022).

4. CBM Collab., *Technical Design Report for the CBM Silicon Tracking System (STS)* (GSI, Darmstadt, 2013). https://repository.gsi.de/record/54798/.

5. A. V. Baranov, D. Dementev, V. Elsha, J. Heuser, P. I. Kharlamov, I. M. Kovalev, A. Kolzhvari, I. A. Kudryashov, A. A. Kurganov, E. Lavrik, V. V. Leontyev, T. Lygdenova, Y. Merkin, M. M. Murin, and J. Panasenko, "The silicon tracking system as part of the hybrid tracker of the BM@N experiment: Technical design report," (JINR, Dubna, 2020). http://www1.jinr.ru/Books/The%20Silicon%20Tracking%20System_sajt.pdf.http://www1.jinr.ru/Books/The%20Silicon%20Tracking%20System_sajt.pdf.

6. V. Blobel, "Software alignment for tracking detectors," Nucl. Instrum. Methods Phys. Res., Sect. A **566**, 5−13 (2006).

7. V. Blobel, "Alignment algorithms," in *Proceedings of the First LHC Detector Alignment Workshop, 2007*, pp. 5−12.

8. A. Voronin, A. Sheremetev, and O. Chikalov, "Production and gluing of the L-legs for the silicon sensors: CBM progress report (2016)," (GSI, Darmstadt, 2017). https://repository.gsi.de/record/201318.

9. A. van den Brink, D. J. van den Broek, L. J. Kok, G-J. L. Nooren, G. A. Feofilov, S. N. Igolkin, F. Daudo, and G. Giraudo, "Tests of prototype ITS-SSD ladder and fixators," ALICE Note INT 2000-04. http://cds.cern.ch/record/689315/files/.

*Translated by I. Obrezanova*